MAGiC

… more of the Science Cases …

Emergent phenomena and topological states in frustrated magnets

with input from Yixi Su

Functional magnetic materials

with input from Michel Kenzelmann and Manuel Angst

- **Complexity in frustrated magnets**
  - ➢ frustration, correlation and competing interactions
  - ➢ ground-state degeneracy -> highly entropic states
  - ➢ topology -> novel topological states

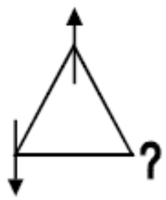

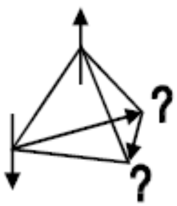

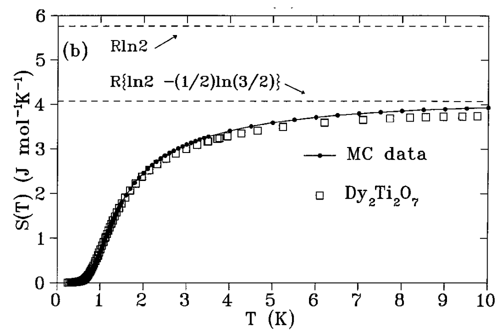

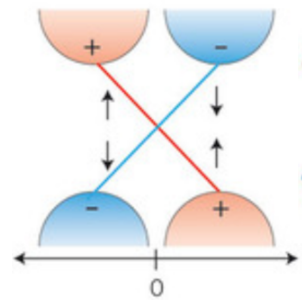

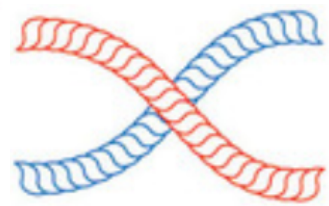

- **Emergent phenomena and topological states**
  - ➢ fractionalization: emergent magnetic monopoles
  - ➢ long range entanglement: quantum spin liquids
  - ➢ topological order: spin-orbit entangled correlated electrons

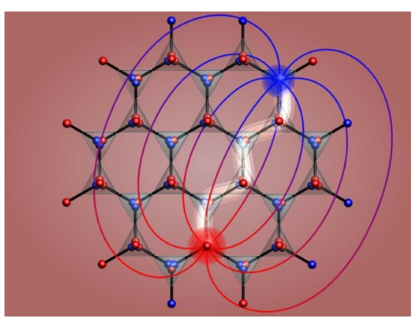

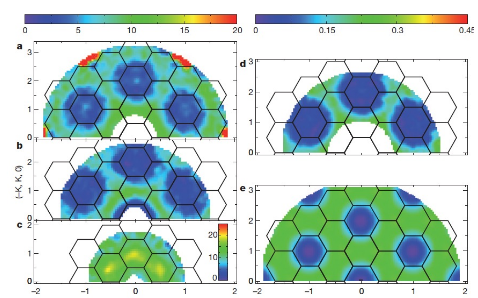

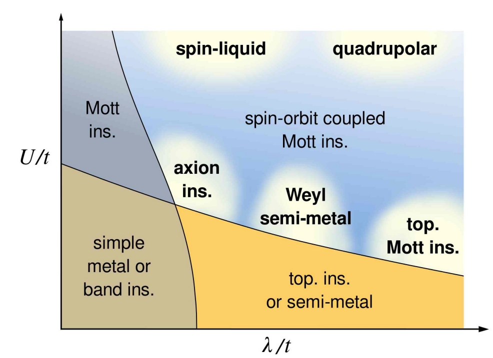

Magnetic Coulomb phase

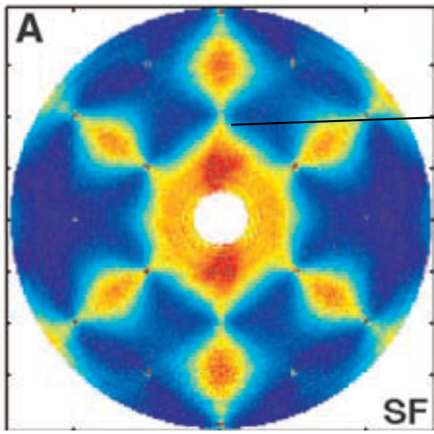

“**Pinch-point singularity**”: indication of dipolar spin correlations due to magnetic Coulomb law

Revealed by polarized single-crystal neutron scattering

Spin ice $Ho_2Ti_2O_7$

T. Fennell, *et al.,* Science **326**, 415 (2009)

D7@ILL

Magnetic Coulomb phase

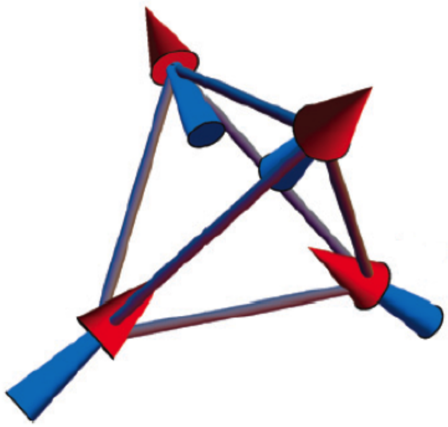

mapping of the “ice rule”
on the diamond lattice

magnetic moments as “flux”
vector field in lattice models

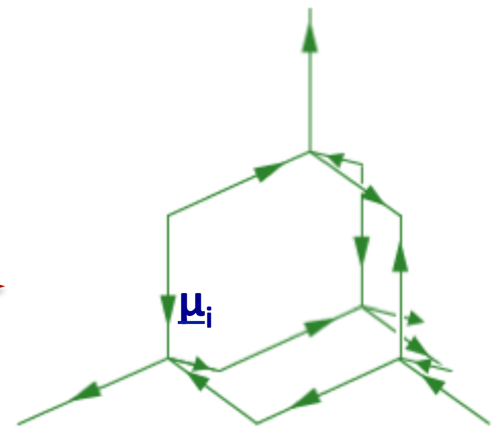

- “ice-rule” local constrain ↔ $\nabla \cdot \underline{\mu}=0$ (divergence-free flux at each vertex)
- emergent gauge structure
- in reciprocal space: bow-tie motif ↔ pinch-point singularity
- long-distance correlation in real space: dipolar

$$\langle S_i(\mathbf{x}) S_j(0) \rangle \propto \frac{3x_i x_j - r^2 \delta_{ij}}{r^5}.$$

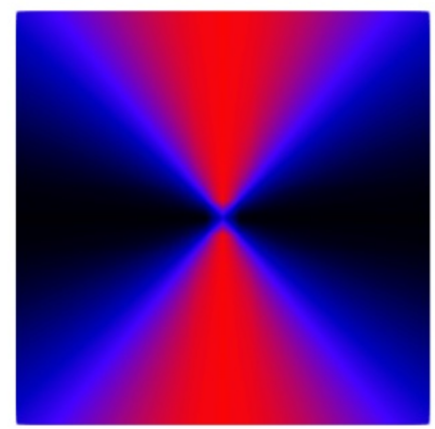

C.L. Henley, Annu. Rev. Condens. Matter Phys. **1**, 179 (2010)

Emergent magnetic monopoles in spin ice

- **Europhysics Prize 2012**
- *Prediction and experimental observation*
  of magnetic monopoles in spin ice
  Bramwell, Castelnovo, Grigera, Moessner, Sondhi, Tennant

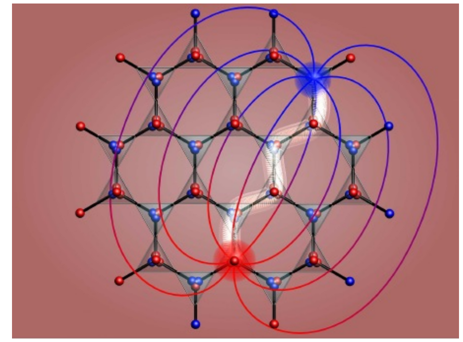

- **Emergent magnetic monopoles in spin ice**
  - fractionalization of magnetic dipoles
  - interact via the magnetic Coulomb law
  - deconfined but connected by the "Dirac string"

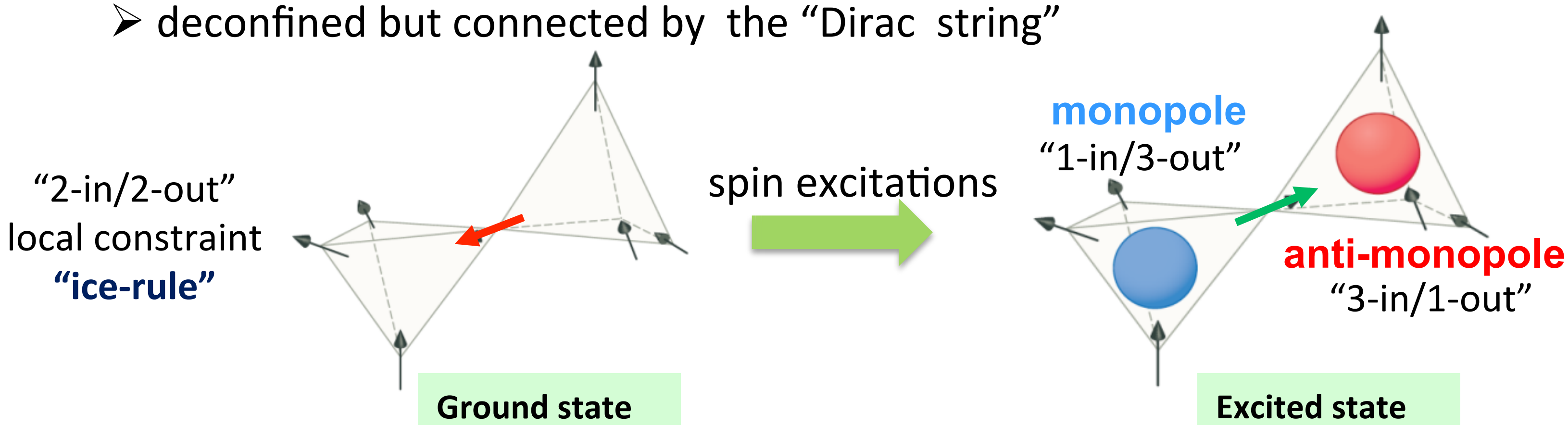

C. Castelnovo, *et al.*, Nature **451**, 42 (2008)
D.J.P. Morris, *et al.*, Science **326**, 411 (2009)
T. Fennell, *et al.*, Science **326**, 415 (2009)

Higgs transition in $Yb_2Ti_2O_7$

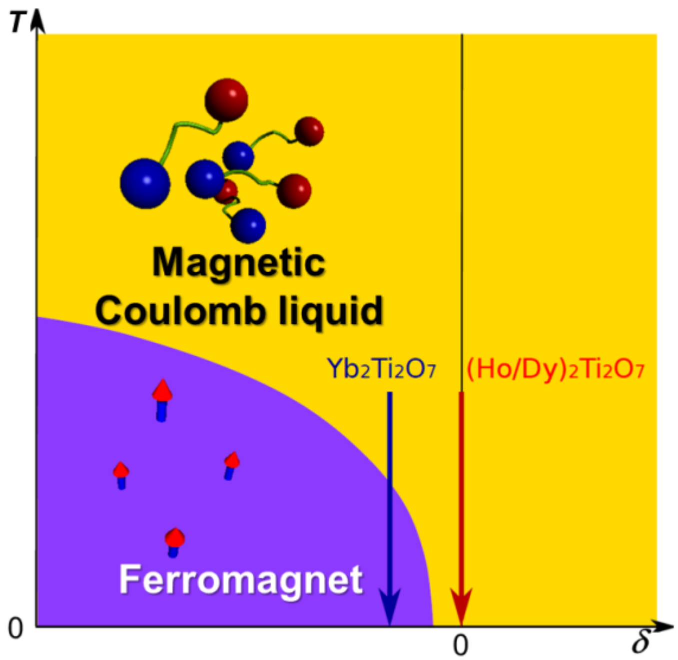

Higgs mechanism in a magnet

Matter fields (*hosted by monopolar spinons*)

+

Dynamical gauge fields (*due to emergent U(1) gauge structure*)

Bose-Einstein condensation
-> spontaneous symmetry breaking
-> a ferromagnet

Higgs transition in $Yb_2Ti_2O_7$

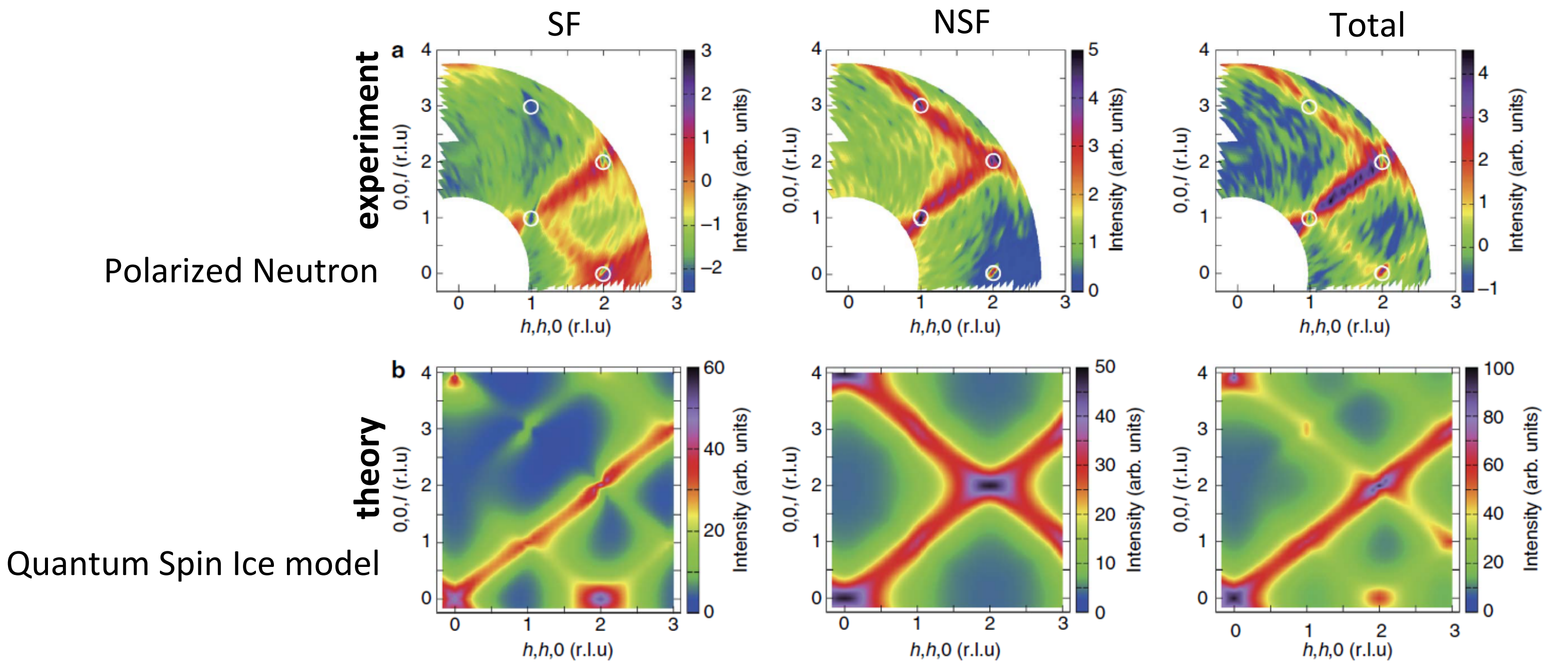

- **High T: a magnetic Coulomb liquid**
  evidence for fractionalized and deconfined monopolar spinons
  i.e. bosonic quasiparticle

L.J. Chang, *et al.,* Nat. Commun. **3**, 992 (2012)

Higgs transition in $Yb_2Ti_2O_7$

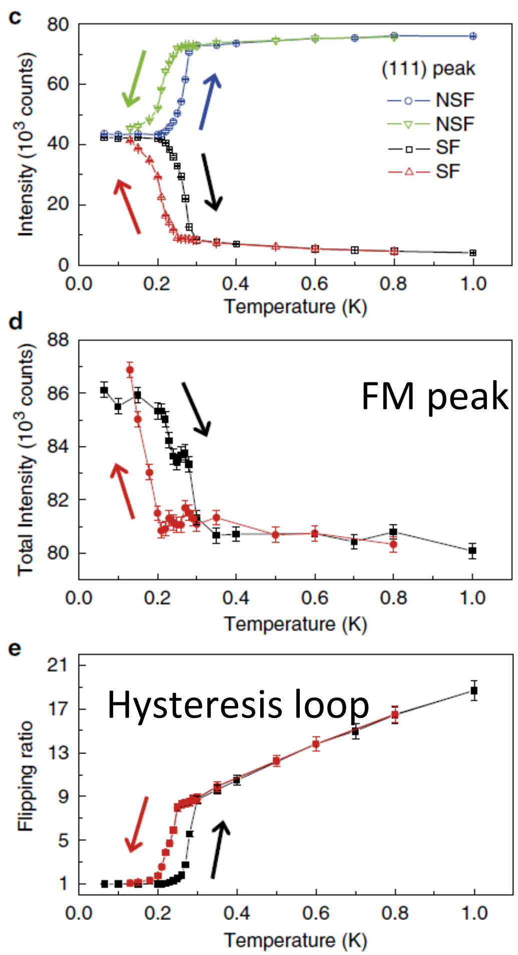

depolarisation

low-T: 1st order transition to ferromagnet

absence of diffuse scattering

ground state: magnetic monopole condensates

i.e. "superconducting" state of magnetic charges

L.J. Chang, *et al.,* Nat. Commun. **3**, 992 (2012)

Possible quantum melting of classical spin ice

nature physics
LETTERS
PUBLISHED ONLINE: 7 APRIL 2013 | DOI: 10.1038/NPHYS2591

Absence of Pauling's residual entropy in thermally equilibrated $Dy_2Ti_2O_7$

D. Pomaranski[1,2,3], L. R. Yaraskavitch[1,2,3], S. Meng[1,2,3], K. A. Ross[4,5], H. M. L. Noad[4,5], H. A. Dabkowska[4,5], B. D. Gaulin[4,5,6] and J. B. Kycia[1,2,3]*

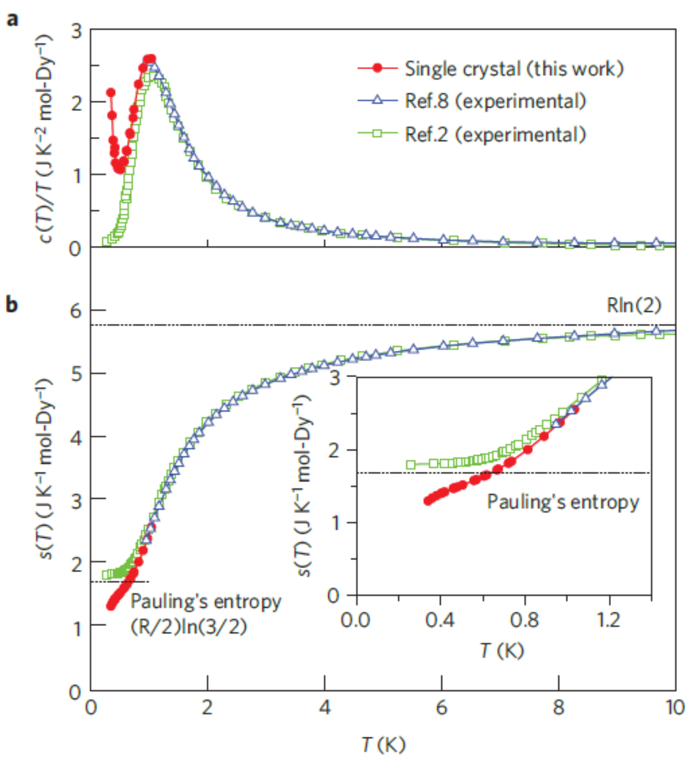

Magnetic ground state of spin ice

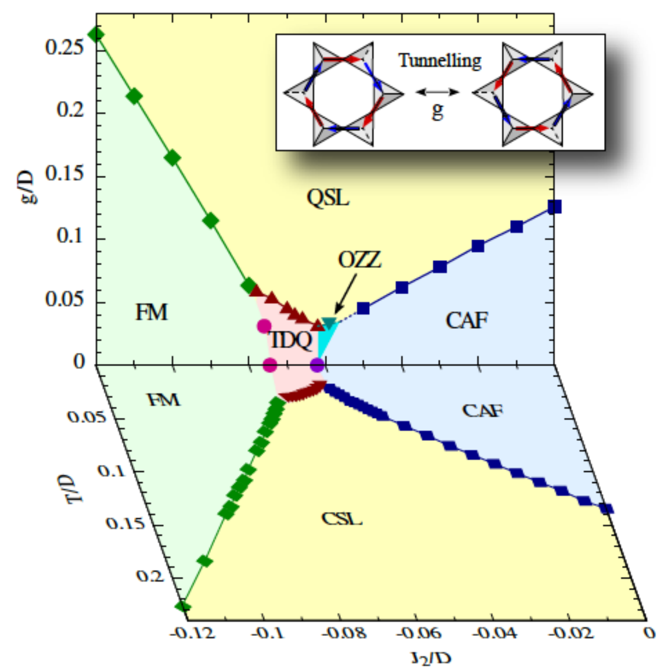

What is the quantum ground state of dipolar spin ice?

P. A. McClarty,[1,2] O. Sikora,[3,4,5] R. Moessner,[2] K. Penc,[6] F. Pollmann,[2] and N. Shannon[4,5]

Magnetic ground state of pyrochlore iridates

Pyrochlore iridates $RE_2Ir_2O_7$

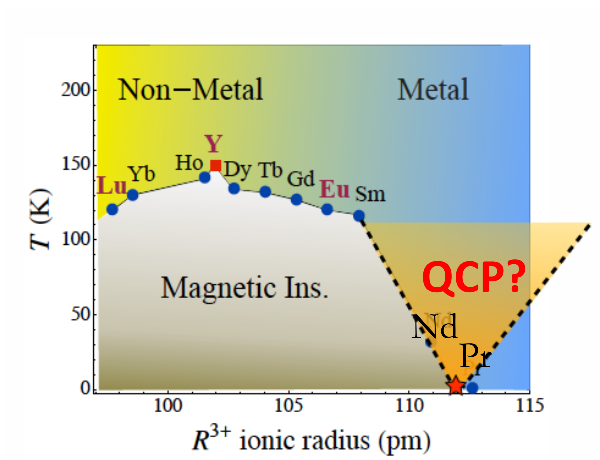

Coulomb repulsion

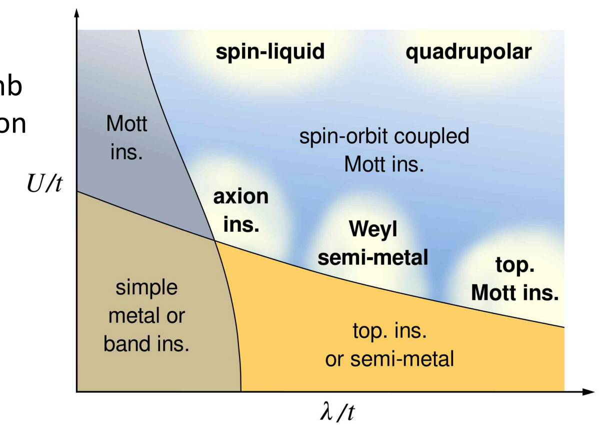

Spin-orbit coupling

… high for Ir

Ir total moment 0.2 to 0.5μB

<u>Key challenges</u>:

- origin of metal-to-insulator transition
- possible presence of quantum criticality
- magnetic order of Ir-sublattice
- emergent topological states

LETTER

doi:10.1038/nature11659

Fractionalized excitations in the spin-liquid state of a kagome-lattice antiferromagnet

Tian-Heng Han[1], Joel S. Helton[2], Shaoyan Chu[3], Daniel G. Nocera[4], Jose A. Rodriguez-Rivera[2,5], Collin Broholm[2,6] & Young S. Lee[1]

Fractionalized excitations in kagome Quantum Spin Liquid

$ZnCu_3(OD)_6Cl_2$

herbertsmithite 1[st] crystal

MACS
@NIST

6 meV

2 meV

0.75 meV

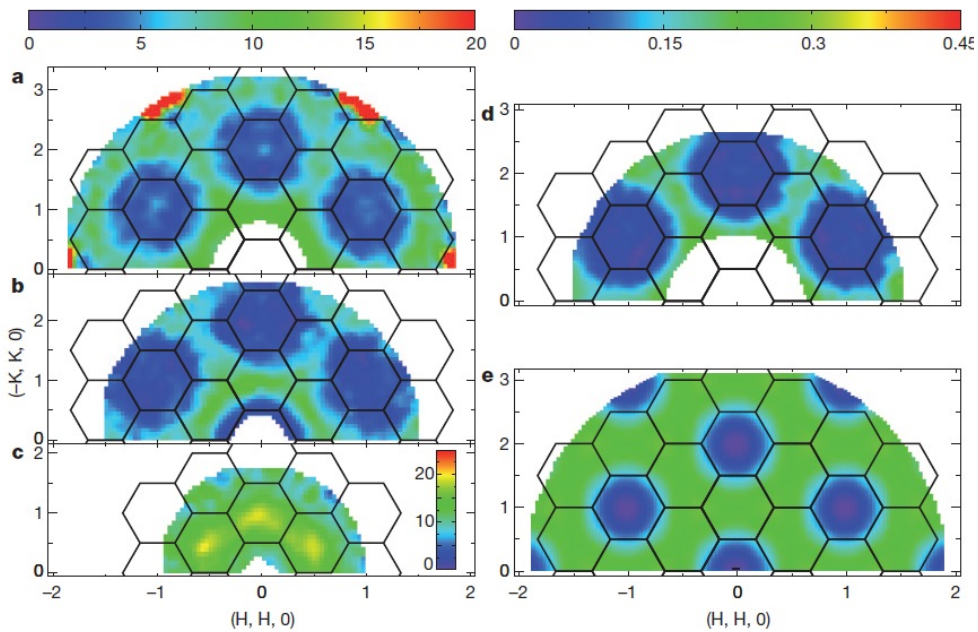

1 to 9 meV

NN dimer model

MAGiC

… more of the Science Cases …

Emergent phenomena and topological states in frustrated magnets

with input from Yixi Su

Functional magnetic materials

with input from Michel Kenzelmann and Manuel Angst “accidental” multiferroic

$BiFeO_3$

Antiferromagnetic below 643 K

Lone-pair ferroelectricity
below 1100 K

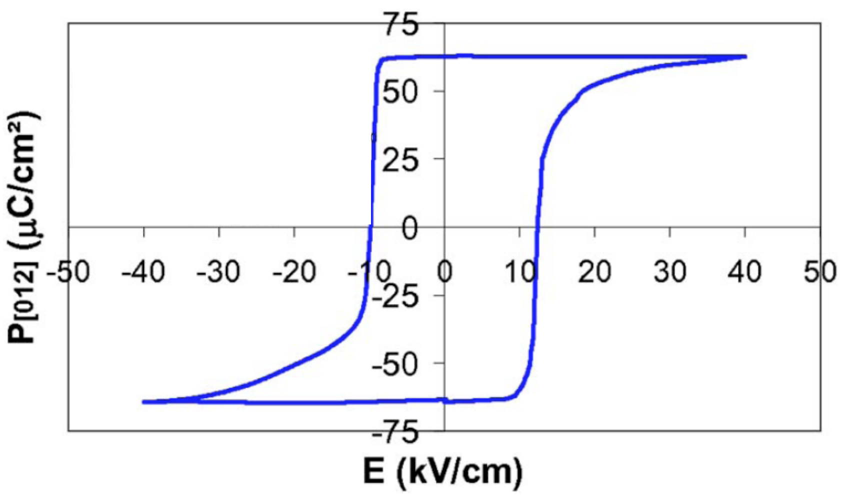

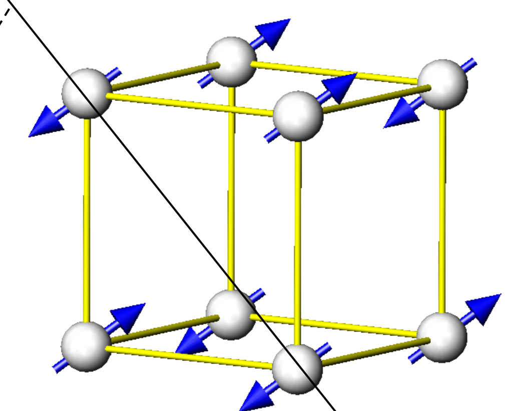

G-type

+small canting
+long-period spiral

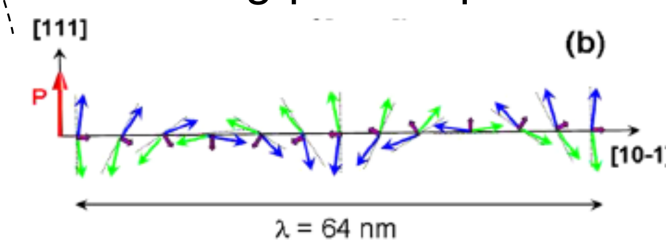

(114 unit cells)

(compare: „traditional“ ferroelectric
$BaTiO_3$ has polarization of ~15 μC/cm^2)

Similar to $BiMnO_3$ – except AF instead of FM.
Also weak magnetoelectric coupling ?

E-control of *M* in $BiFeO_3$

Experimentally verified by Lebeugle *et al*. [PRL 100, 227602 (2008)]

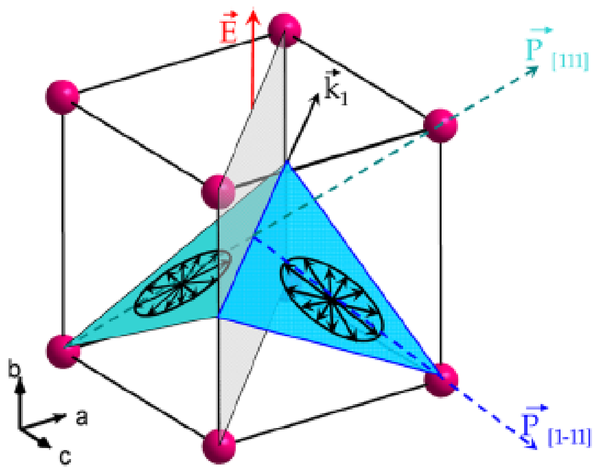

With exchange bias, control of ***M*** in a neighboring soft ferromagnet

Chu *et al*. [Nat. Mater. 7, 478 (2008)] Demonstrated even this, using CoFe on $BiFeO_3$

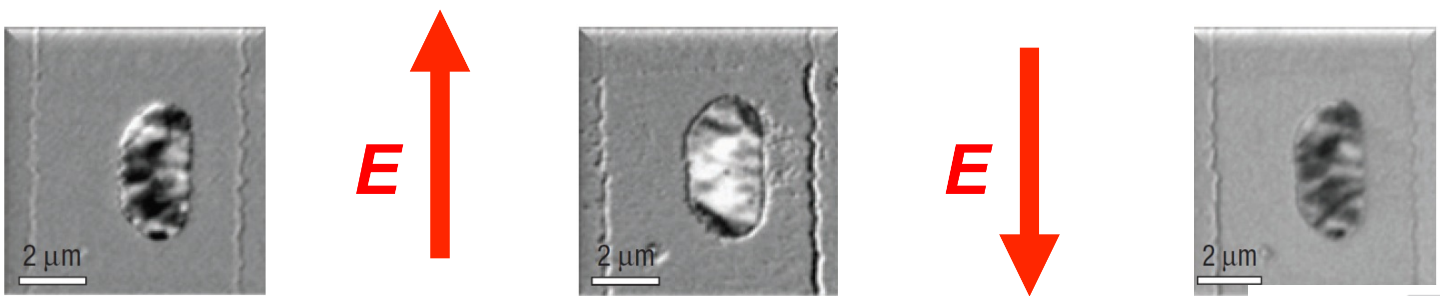

Experiment at Room temperature

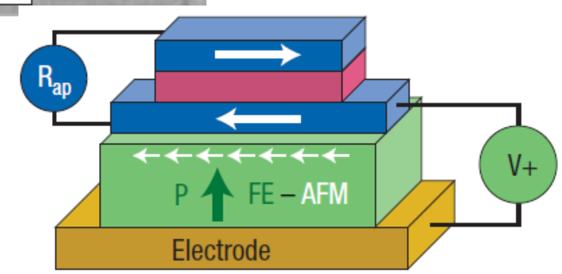

Spin spiral ferroelectricity: $TbMnO_3$

Observation of a polarization in **$TbMnO_3$** (distorted perovskite-structure) by Kimura *et al*. [Nature **426**, 55 (2003)] started a boom in multiferroics research

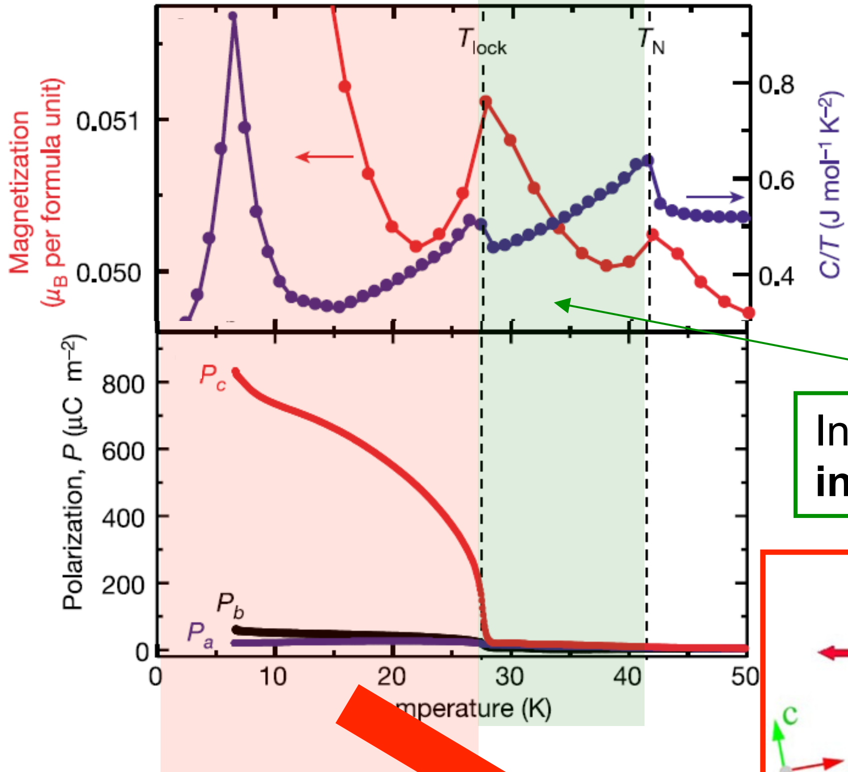

Incommensurate, almost collinear, and **inversion symmetric** spin structure

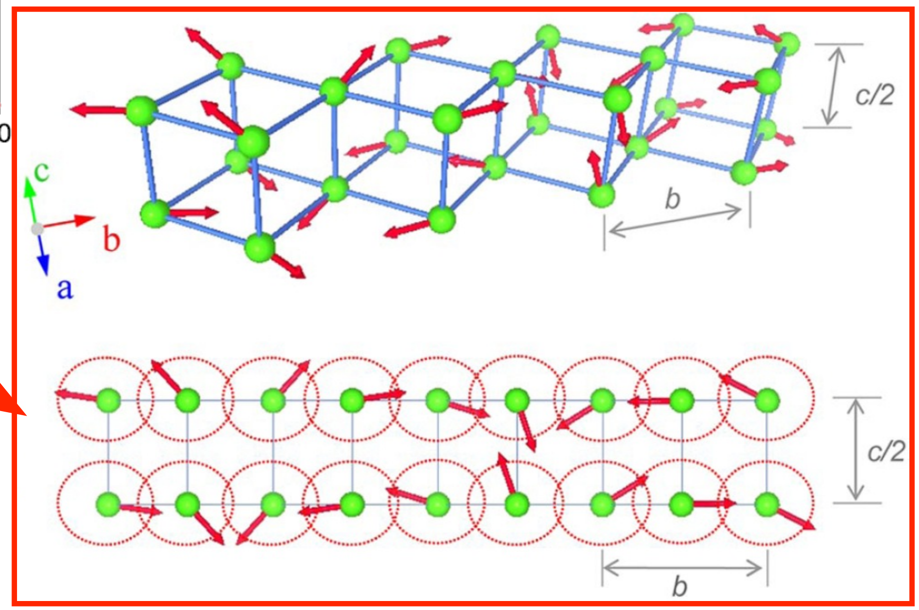

Below 26 K cycloidal spin structure:

- spins rotate in *bc*-plane
- breaks inversion-symmetry!

  → allows electric polarization

Magnetoelectric coupling

Spin-spirals : no net magnetization that could be switched –
but sense of rotation along spiral is connected to the polarization.

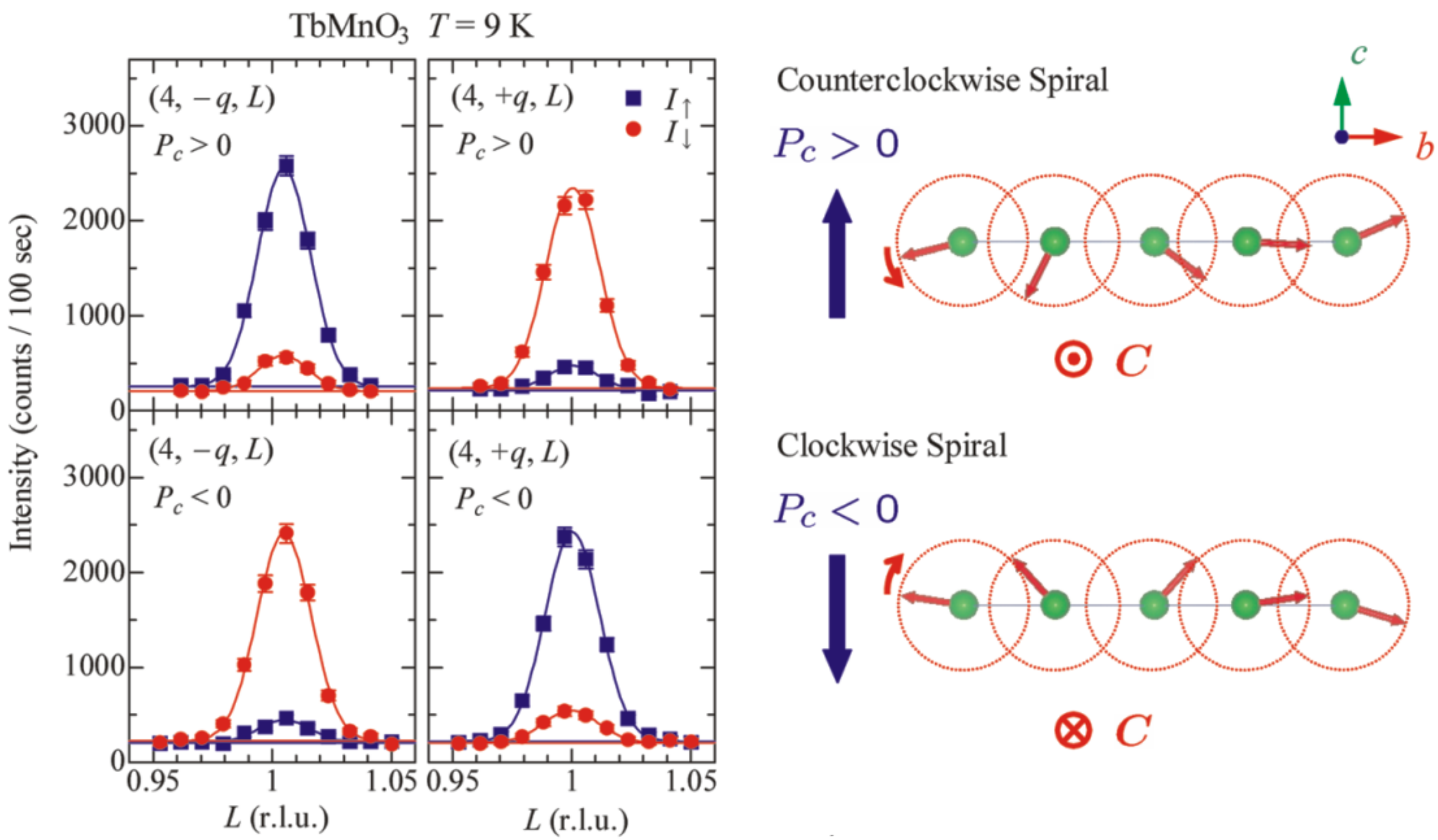

Verified for $TbMnO_3$ by polarized neutron diffraction after cooling in +/- *E*-field.

Switching within the FE state was not possible, however.

Prediction of strain-induced ferroelectricity

Prediction of a magnetic and electric phase with magneto-electric coupling for $EuTiO_3$ under epitaxial strain

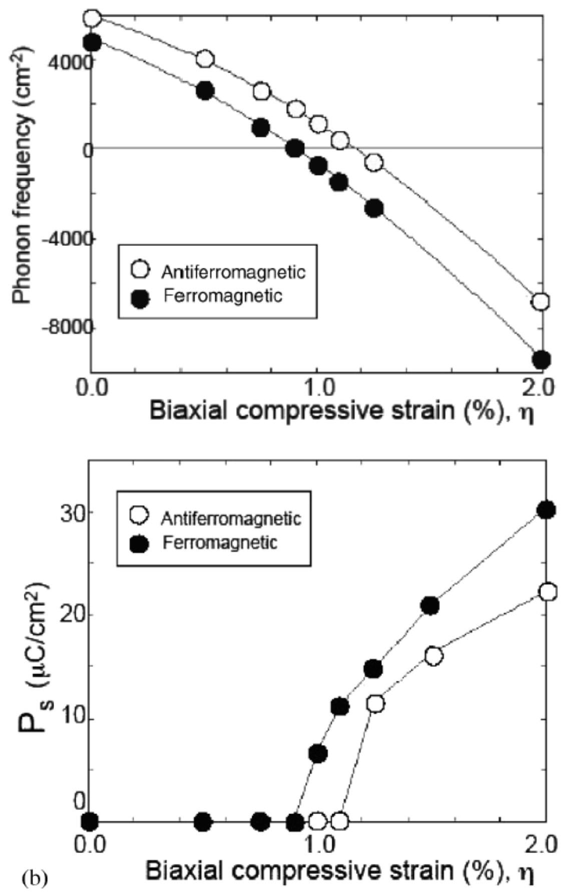

C.J. Fennie and K.M. Rabe, Phys. Rev. Lett. **97**, 267602 (2006).

Strong ferroelectric ferromagnetic due to spin-lattice coupling

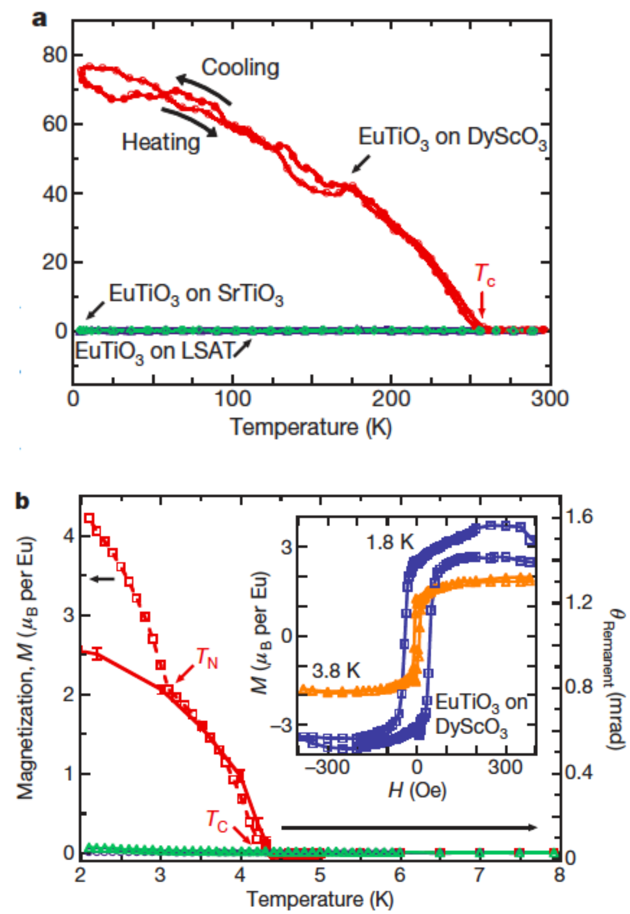

J.H. Lee et al, Nature **466**, 9331 (2010).

Novel multiferroicity

Ferroelectricity from rotations?

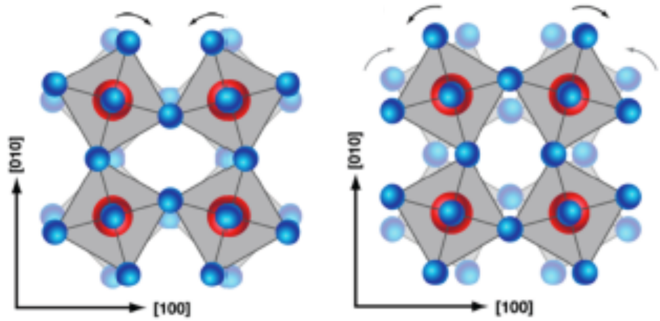

G. Lawes Physics **4** 18 2011

Possible for more complex perovskite-based structures

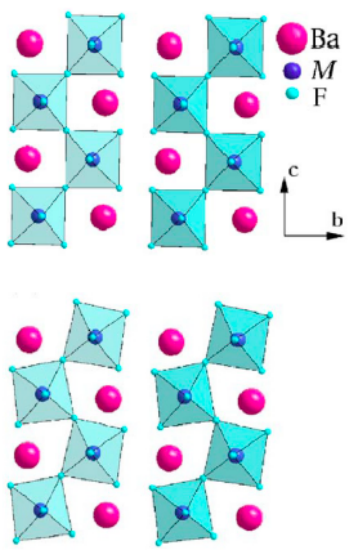

C. Ederer and N.A. Spaldin, Phys. Rev. B 74 , 024102 (2006)

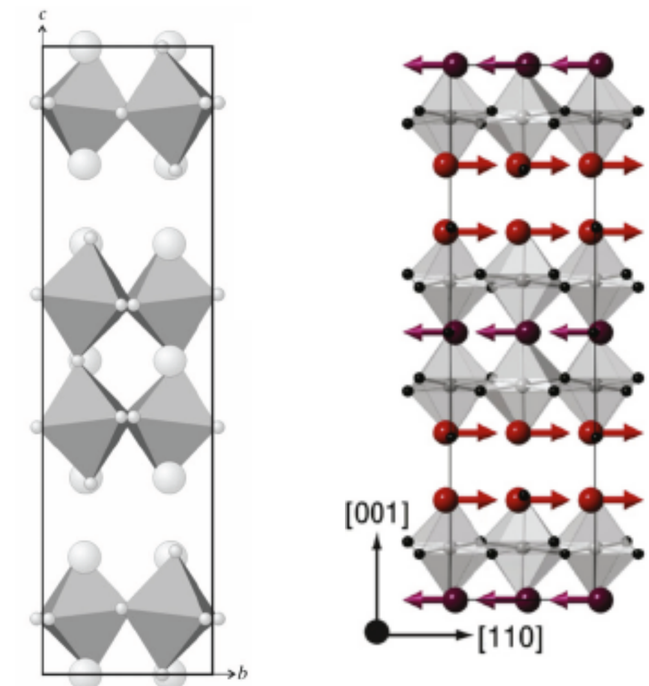

N.A. Benedek and C.J. Fennie, Phys. Rev. Lett **106** 107204 (2011)

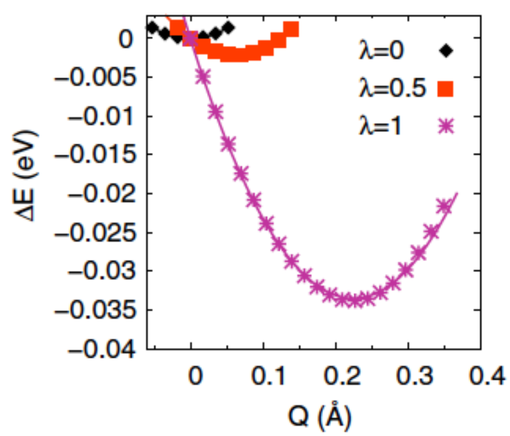

Lower energy for coupled mode involving ferroelectricity

Neutron scattering of 90 nm o-$LuMnO_3$ thin film

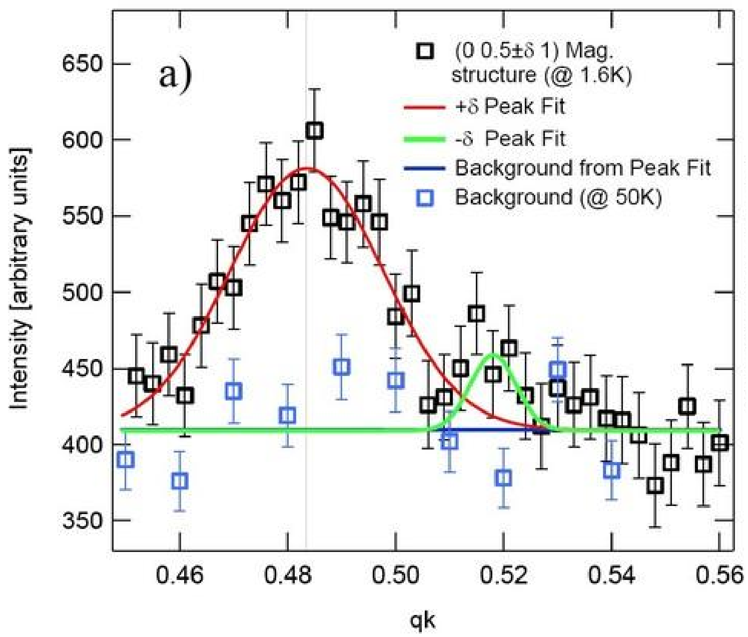

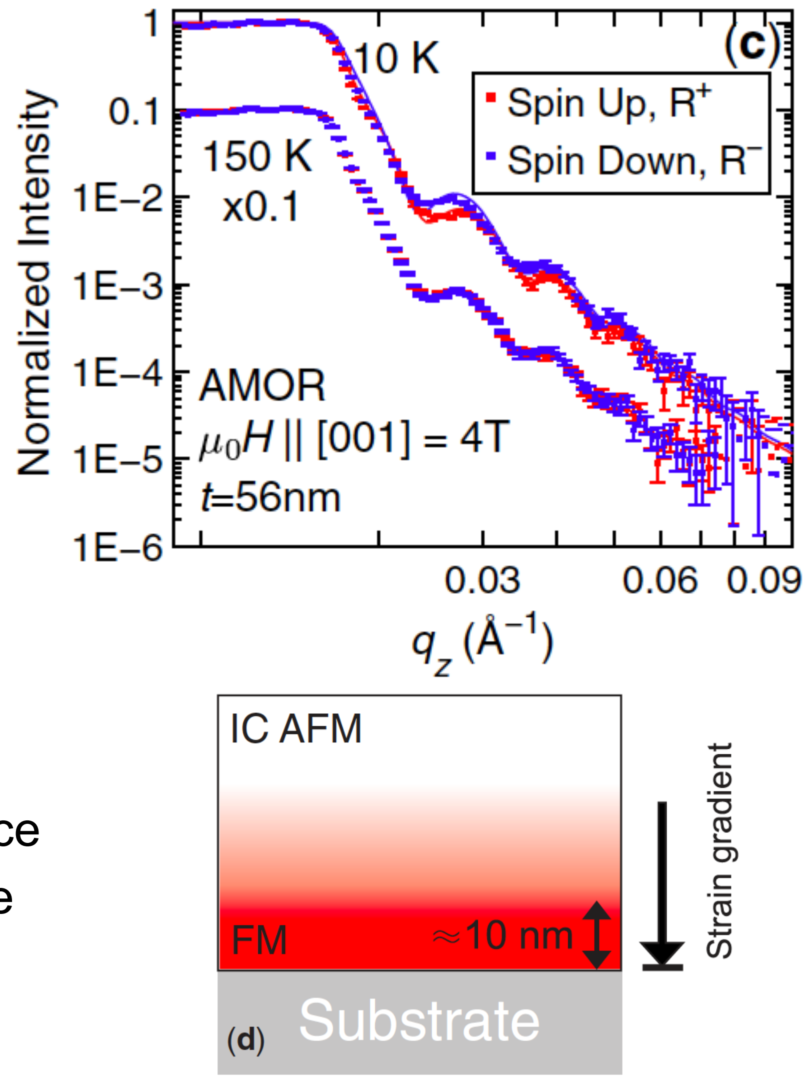

Antiferromagnetic towards surface

Ferromagnetic towards substrate

Switching of SDW domains in a d-wave superconductor

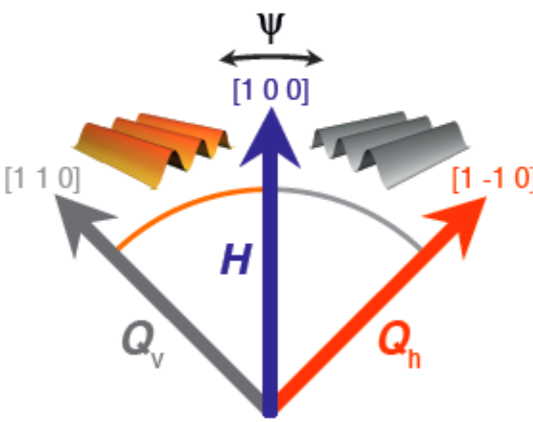

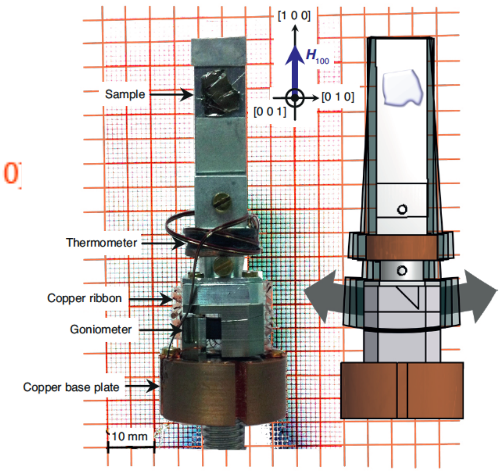

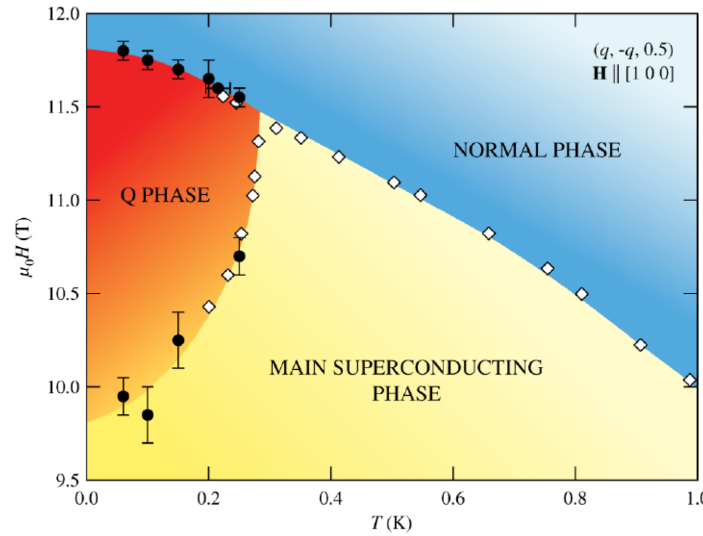

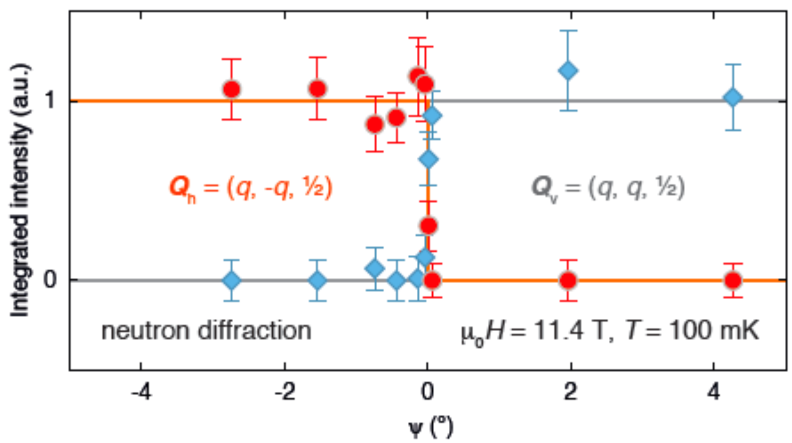

Sharp switching provides evidence for presence of p-wave pair density wave in Q-phase

S. Gerber et al, Nature Physics **10**, 126 (2014)

MAGiC

Science Cases

=> resulting requests for the instrument

Concept

Diffuse **and** Bragg scattering

sufficient Q-resolution for incommensurate structures

magnetic structure determination

- bispectral
- homogeneous response of analyzer & detector 1mm

Polarized neutrons

either half-polarized or with polarization analysis

- permanent by supermirrors and guide optics

TOF-Laue

3D resolution and flexible large Q-space

- continuous rotation & event mode

Blume 1963 , Maleyev 1958-1961

Scattering and Polarization

$$\sigma_{\mathbf{Q}} = \sigma^{\mathbf{N}}_{\mathbf{Q},\mathrm{coh}} + \sigma^{\mathbf{N}}_{\mathbf{Q},\mathrm{isotope\text{-}inc}} + \sigma^{\mathbf{N}}_{\mathbf{Q},\mathrm{spin\text{-}inc}}$$

nuclear

$$\sigma^{\mathbf{N}}_{\mathbf{Q},\mathrm{coh}} = |N_{\mathbf{Q}}|^2$$

$$+ |\mathbf{M}^{\perp}_{\mathbf{Q}}|^2 + \mathbf{P}(N_{-\mathbf{Q}}\mathbf{M}^{\perp}_{\mathbf{Q}} + \mathbf{M}^{\perp}_{-\mathbf{Q}}N_{\mathbf{Q}}) + i\mathbf{P}(\mathbf{M}^{\perp}_{-\mathbf{Q}} \times \mathbf{M}^{\perp}_{\mathbf{Q}})$$

magnetic *magnetic-nuclear interference* *chirality*

"half-polarised"

$$\mathbf{P}'\sigma_{\mathbf{Q}} = \mathbf{P}\sigma^{\mathbf{N}}_{\mathbf{Q},\mathrm{coh}} + \mathbf{P}\sigma^{\mathbf{N}}_{\mathbf{Q},\mathrm{isotop\text{-}inc}} - \tfrac{1}{3}\mathbf{P}\sigma^{\mathbf{N}}_{\mathbf{Q},\mathrm{spin\text{-}inc}}$$
$$+\mathbf{M}^{\perp}_{\mathbf{Q}}(\mathbf{P}\mathbf{M}^{\perp}_{-\mathbf{Q}}) + \mathbf{M}^{\perp}_{-\mathbf{Q}}(\mathbf{P}\mathbf{M}^{\perp}_{\mathbf{Q}}) - \mathbf{P}\mathbf{M}^{\perp}_{\mathbf{Q}}\mathbf{M}^{\perp}_{-\mathbf{Q}}$$
$$+\mathbf{M}^{\perp}_{\mathbf{Q}}N_{-\mathbf{Q}} + \mathbf{M}^{\perp}_{-\mathbf{Q}}N_{\mathbf{Q}} + i(\mathbf{M}^{\perp}_{\mathbf{Q}}N_{-\mathbf{Q}} - \mathbf{M}^{\perp}_{-\mathbf{Q}}N_{\mathbf{Q}}) \times \mathbf{P} + i\mathbf{M}^{\perp}_{\mathbf{Q}} \times \mathbf{M}^{\perp}_{-\mathbf{Q}}$$

Blume 1963 , Maleyev 1958-1961

Scattering and Polarization

$$\sigma_{\mathbf{Q}} = \sigma^{\mathbf{N}}_{\mathbf{Q},\mathrm{coh}} + \sigma^{\mathbf{N}}_{\mathbf{Q},\mathrm{isotope\text{-}inc}} + \sigma^{\mathbf{N}}_{\mathbf{Q},\mathrm{spin\text{-}inc}}$$

nuclear

$$\sigma^{\mathbf{N}}_{\mathbf{Q},\mathrm{coh}} = |N_{\mathbf{Q}}|^2$$

$$+ |\mathbf{M}^{\perp}_{\mathbf{Q}}|^2 + \mathbf{P}(N_{-\mathbf{Q}}\mathbf{M}^{\perp}_{\mathbf{Q}} + \mathbf{M}^{\perp}_{-\mathbf{Q}}N_{\mathbf{Q}}) + i\mathbf{P}(\mathbf{M}^{\perp}_{-\mathbf{Q}} \times \mathbf{M}^{\perp}_{\mathbf{Q}})$$

magnetic *magnetic-nuclear interference* *chirality*

$\mathbf{x} \parallel \mathbf{Q}$

$\mathbf{P_z} \rightarrow -\mathbf{P_z}$ $\mathbf{NM_z}$

$\mathbf{P_y} \rightarrow -\mathbf{P_y}$ $\mathbf{NM_y}$

$$\mathbf{P}'\sigma_{\mathbf{Q}} = \mathbf{P}\sigma^{\mathbf{N}}_{\mathbf{Q},\mathrm{coh}} + \mathbf{P}\sigma^{\mathbf{N}}_{\mathbf{Q},\mathrm{isotop\text{-}inc}} - \tfrac{1}{3}\mathbf{P}\sigma^{\mathbf{N}}_{\mathbf{Q},\mathrm{spin\text{-}inc}}$$

$$+\mathbf{M}^{\perp}_{\mathbf{Q}}(\mathbf{P}\mathbf{M}^{\perp}_{-\mathbf{Q}}) + \mathbf{M}^{\perp}_{-\mathbf{Q}}(\mathbf{P}\mathbf{M}^{\perp}_{\mathbf{Q}}) - \mathbf{P}\mathbf{M}^{\perp}_{\mathbf{Q}}\mathbf{M}^{\perp}_{-\mathbf{Q}}$$

$$+\mathbf{M}^{\perp}_{\mathbf{Q}}N_{-\mathbf{Q}} + \mathbf{M}^{\perp}_{-\mathbf{Q}}N_{\mathbf{Q}} + i(\mathbf{M}^{\perp}_{\mathbf{Q}}N_{-\mathbf{Q}} - \mathbf{M}^{\perp}_{-\mathbf{Q}}N_{\mathbf{Q}}) \times \mathbf{P} + i\mathbf{M}^{\perp}_{\mathbf{Q}} \times \mathbf{M}^{\perp}_{-\mathbf{Q}}$$

applied fields H,E

Blume 1963 , Maleyev 1958-1961

Functional magnetic materials, Multiferroics,
Molecular Magnetism, spin density - anisotropy

Scattering and Polarization

$$\sigma_{\mathbf{Q}} = \sigma^{\mathbf{N}}_{\mathbf{Q},\mathrm{coh}} + \sigma^{\mathbf{N}}_{\mathbf{Q},\mathrm{isotope\text{-}inc}} + \sigma^{\mathbf{N}}_{\mathbf{Q},\mathrm{spin\text{-}inc}}$$ *nuclear* $$\sigma^{\mathbf{N}}_{\mathbf{Q},\mathrm{coh}} = |N_{\mathbf{Q}}|^2$$

$$+|\mathbf{M}^{\perp}_{\mathbf{Q}}|^2 + \mathbf{P}(N_{-\mathbf{Q}}\mathbf{M}^{\perp}_{\mathbf{Q}} + \mathbf{M}^{\perp}_{-\mathbf{Q}}N_{\mathbf{Q}}) + i\mathbf{P}(\mathbf{M}^{\perp}_{-\mathbf{Q}} \times \mathbf{M}^{\perp}_{\mathbf{Q}})$$

magnetic *magnetic-nuclear interference* *chirality* $\mathbf{S} \times \mathbf{S}'$

$\mathbf{x} \parallel \mathbf{Q}$

$\mathbf{P_z} \rightarrow -\mathbf{P_z}$ $\mathbf{NM_z}$

$\mathbf{P_y} \rightarrow -\mathbf{P_y}$ $\mathbf{NM_y}$

$\mathbf{P_x} \rightarrow -\mathbf{P_x}$

$\mathbf{q} \parallel \mathbf{Q}$ *helix*

$\mathbf{q} \perp \mathbf{Q}$ *cycloid*

$$\mathbf{P}'\sigma_{\mathrm{Q}} = \mathbf{P}\sigma^{\mathrm{N}}_{\mathrm{Q,coh}} + \mathbf{P}\sigma^{\mathrm{N}}_{\mathrm{Q,isotop\text{-}inc}} - \tfrac{1}{3}\mathbf{P}\sigma^{\mathrm{N}}_{\mathrm{Q,spin\text{-}inc}}$$

$$+\mathbf{M}^{\perp}_{\mathrm{Q}}(\mathbf{P}\mathbf{M}^{\perp}_{-\mathrm{Q}}) + \mathbf{M}^{\perp}_{-\mathrm{Q}}(\mathbf{P}\mathbf{M}^{\perp}_{\mathrm{Q}}) - \mathbf{P}\mathbf{M}^{\perp}_{\mathrm{Q}}\mathbf{M}^{\perp}_{-\mathrm{Q}}$$

$$+\mathbf{M}^{\perp}_{\mathrm{Q}}N_{-\mathrm{Q}} + \mathbf{M}^{\perp}_{-\mathrm{Q}}N_{\mathrm{Q}} + i(\mathbf{M}^{\perp}_{\mathrm{Q}}N_{-\mathrm{Q}} - \mathbf{M}^{\perp}_{-\mathrm{Q}}N_{\mathrm{Q}}) \times \mathbf{P} + i\mathbf{M}^{\perp}_{\mathrm{Q}} \times \mathbf{M}^{\perp}_{-\mathrm{Q}}$$

Blume 1963 , Maleyev 1958-1961

Scattering and Polarization

$$\sigma_{\mathbf{Q}} = \sigma^{\mathbf{N}}_{\mathbf{Q},\mathrm{coh}} + \sigma^{\mathbf{N}}_{\mathbf{Q},\mathrm{isotope\text{-}inc}} + \sigma^{\mathbf{N}}_{\mathbf{Q},\mathrm{spin\text{-}inc}}$$ *nuclear* $$\sigma^{\mathbf{N}}_{\mathbf{Q},\mathrm{coh}} = |N_{\mathbf{Q}}|^2$$

$$+|\mathbf{M}^{\perp}_{\mathbf{Q}}|^2 + \mathbf{P}(N_{-\mathbf{Q}}\mathbf{M}^{\perp}_{\mathbf{Q}} + \mathbf{M}^{\perp}_{-\mathbf{Q}}N_{\mathbf{Q}}) + i\mathbf{P}(\mathbf{M}^{\perp}_{-\mathbf{Q}} \times \mathbf{M}^{\perp}_{\mathbf{Q}})$$

magnetic *magnetic-nuclear interference* *chirality* $\mathbf{S} \times \mathbf{S}'$

$\mathbf{x} \parallel \mathbf{Q}$

$\mathbf{P_z} \to -\mathbf{P_z}$ $\mathrm{NM_z}$

$\mathbf{P_y} \to -\mathbf{P_y}$ $\mathrm{NM_y}$

$\mathbf{P_x} \to -\mathbf{P_x}$

$\mathbf{q} \parallel \mathbf{Q}$ *helix*

$\mathbf{q} \perp \mathbf{Q}$ *cycloid*

$$\mathbf{P}'\sigma_{\mathbf{Q}} = \mathbf{P}\sigma^{\mathbf{N}}_{\mathbf{Q},\mathrm{coh}} + \mathbf{P}\sigma^{\mathbf{N}}_{\mathbf{Q},\mathrm{isotop\text{-}inc}} - \tfrac{1}{3}\mathbf{P}\sigma^{\mathbf{N}}_{\mathbf{Q},\mathrm{spin\text{-}inc}}$$

$$+\mathbf{M}^{\perp}_{\mathbf{Q}}(\mathbf{P}\mathbf{M}^{\perp}_{-\mathbf{Q}}) + \mathbf{M}^{\perp}_{-\mathbf{Q}}(\mathbf{P}\mathbf{M}^{\perp}_{\mathbf{Q}}) - \mathbf{P}\mathbf{M}^{\perp}_{\mathbf{Q}}\mathbf{M}^{\perp}_{-\mathbf{Q}}$$

$$+\mathbf{M}^{\perp}_{\mathbf{Q}}N_{-\mathbf{Q}} + \mathbf{M}^{\perp}_{-\mathbf{Q}}N_{\mathbf{Q}} + i(\mathbf{M}^{\perp}_{\mathbf{Q}}N_{-\mathbf{Q}} - \mathbf{M}^{\perp}_{-\mathbf{Q}}N_{\mathbf{Q}}) \times \mathbf{P} + i\mathbf{M}^{\perp}_{\mathbf{Q}} \times \mathbf{M}^{\perp}_{-\mathbf{Q}}$$

Separate all by longitudinal polarization analysis $N^2,\ M_z^2,\ M_y^2,\ NM_z,\ NM_y,\ M \times M'$

XYZ-polarisation analysis of diffuse magnetic neutron scattering from single crystals W. Schweika 2010 *J. Phys.: Conf. Ser.* **211** 012026.

Neutron optics: polarizing guide + polarizing bispectral switch

FOM	1 cm^2	$+/-0.3^\circ$	thermal
		$+/-0.5^\circ$	cold

… and typically we use most of the ESS pulse

ESS moderator

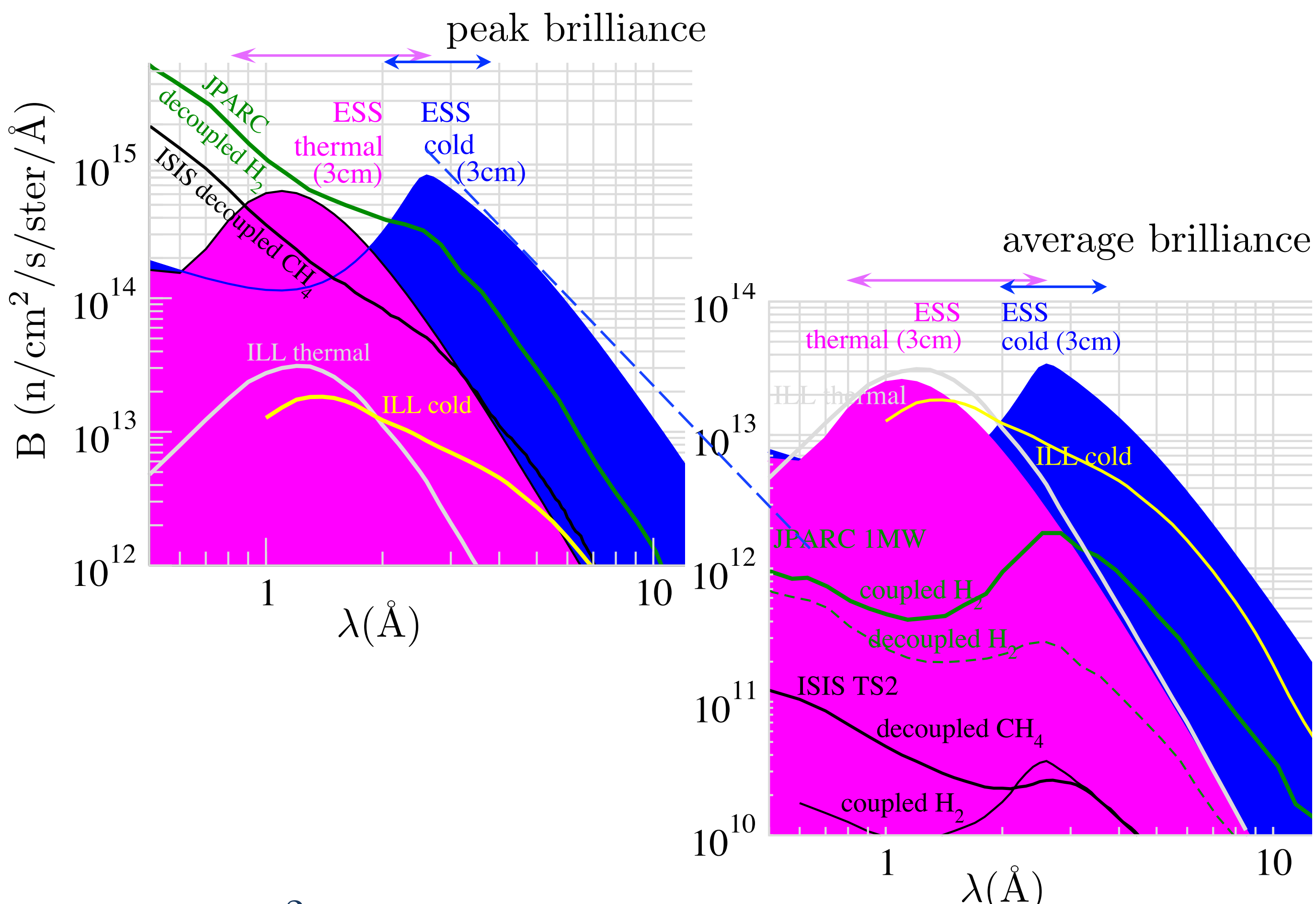

how to compare?

thermal will do also very well

currently, optimization for thermal moderator
comparison to pancake (optimized cold moderator)
yields ~ 2 times more thermal flux and ~ same cold flux

Choppers

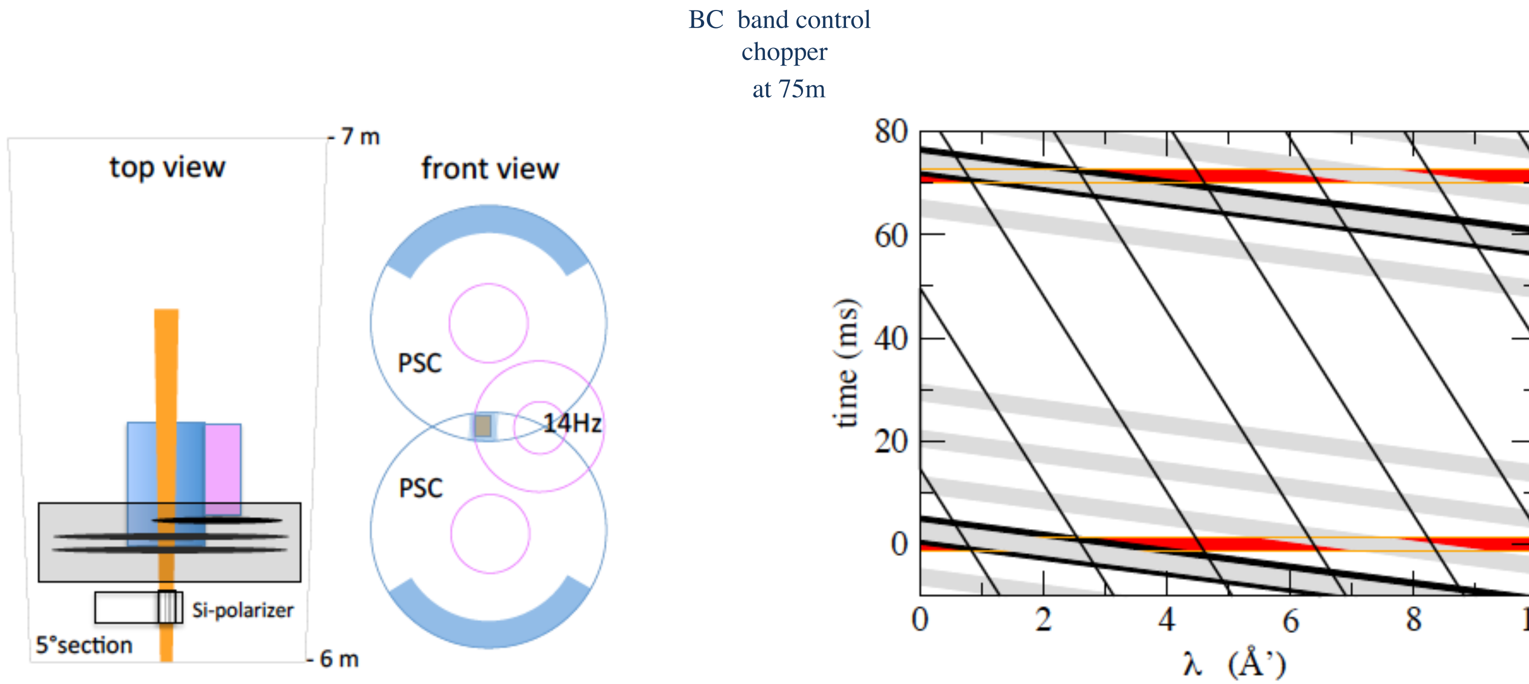

Figure 8. *(left)* The PSC counter rotating system and 14Hz chopper in top and front view. *(right)* Acceptance diagram provides a overview for a clean solution for 0.8Å<λ<2.6Å and a pulse/time-resolution varying with λ as magnified in the inset.

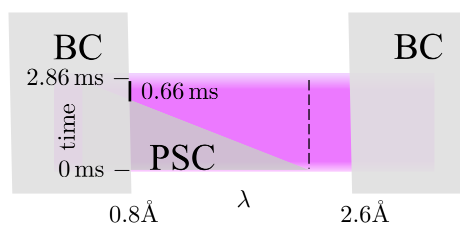

thermal

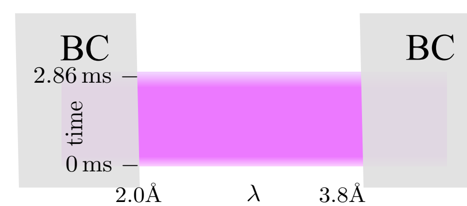

cold

Resolution chopper

Fermi chopper, straight Si wafer slits, at ~50-75cm before sample

opening time t_o=d/v_u, v_u=Pi Lv
neutron TOF t_n=L/v_n
optimize for:

pulse ~20µs (10µs)

t_n<<20µs
t_n=lambda L 2.5*10^{-7} s/mm/Å
\lambda<6Å t_n<10µs
L=6.6mm
d=280µm (140µm)

repetition rate 2\nu =96Hz*14 = 1344Hz
rotation frequency 48 Hz

Pulse suppression \nu' =24 (16,12) x 14 Hz

d/L = 0.042 = 2.43°
⇒ ^{10}B d_a>15µm absorber thickness for 10^{-6} transmission
⇒ Gd d_a> 1µm

Detector

^{10}B absorber   Jalousie-type   (^{3}He alternative)
efficiency >50% at λ =1Å
resolution 3mm x 3mm
no blind areas

vertical   +/- 30°

compatible
with 8T magnet

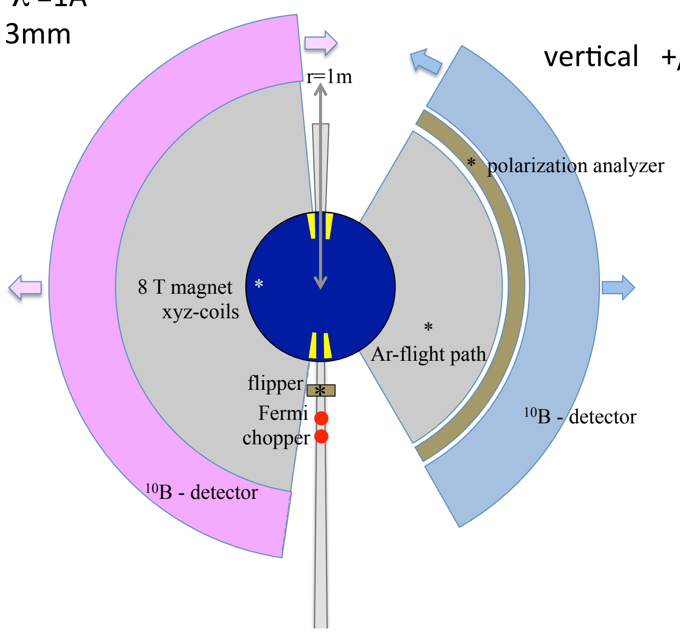

Supermirror polarization analyzer
HYSPEC (built by PSI)

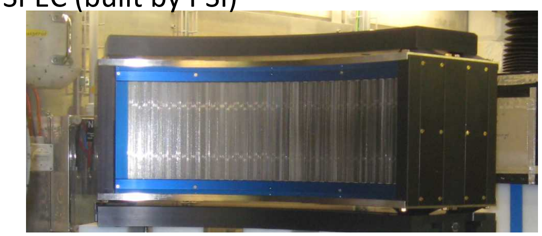

MAGIC analyzer
FeSi - Si-wafer mirror stack
high performance
low divergence (sample / 90 cm distance)
homogeneous response
λ > 2Å
Protoyping (PSI&JCNS)

Why should we go for an inelastic option?

- no compromise for diffraction
- cheap (add 2 Fermi-choppers only; compare to detector of DG TOF)
- most interesting case is not optimized at typical/standard DG TOF
  which have a preference for better resolution particular for QENS
  coherent with ESS suite
- special for polarization, small samples,
  low-T & down-scattering, high Q-resolution

=> very high performance

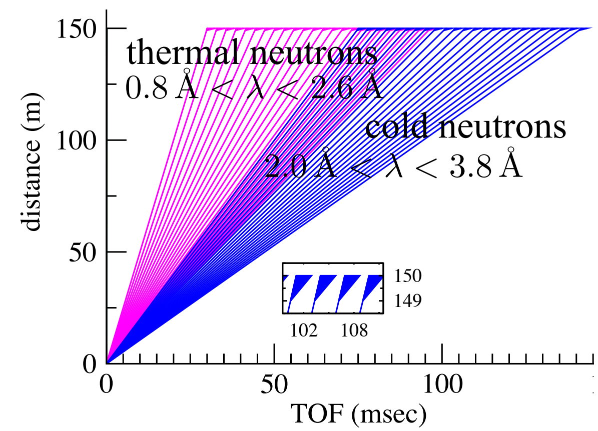

4SEASONS JPARC

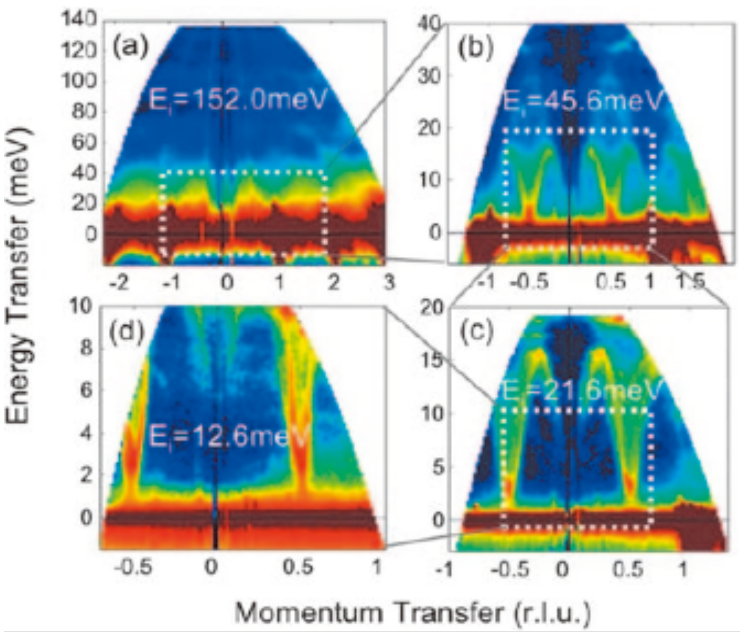

multiple

48SEASONS ESS

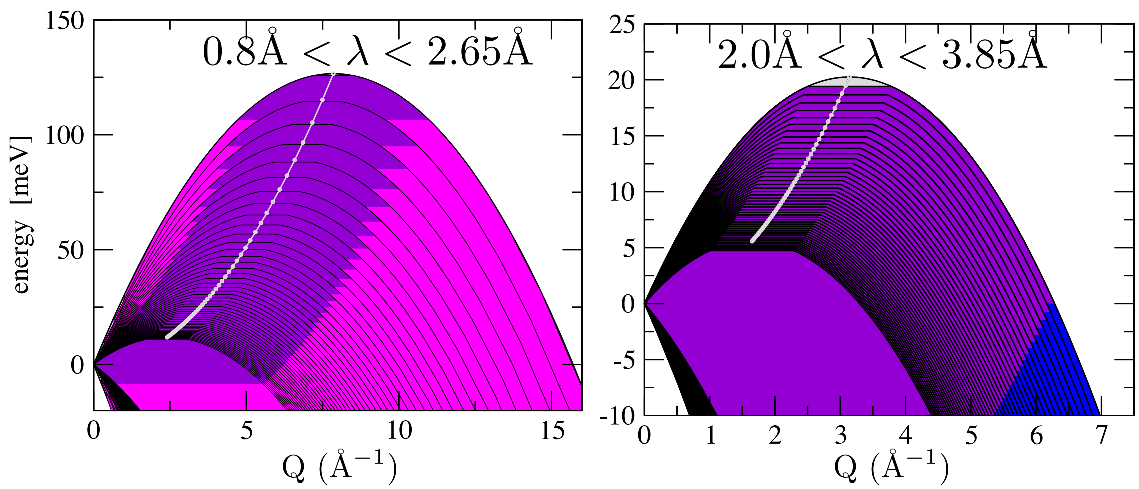

with polarization analysis

Data from 4SEASONS

simultaneous measurements are great (comparisons to ARCS)
current software development to quickly view and orient the data
better Q-resolution would be good (thermal)

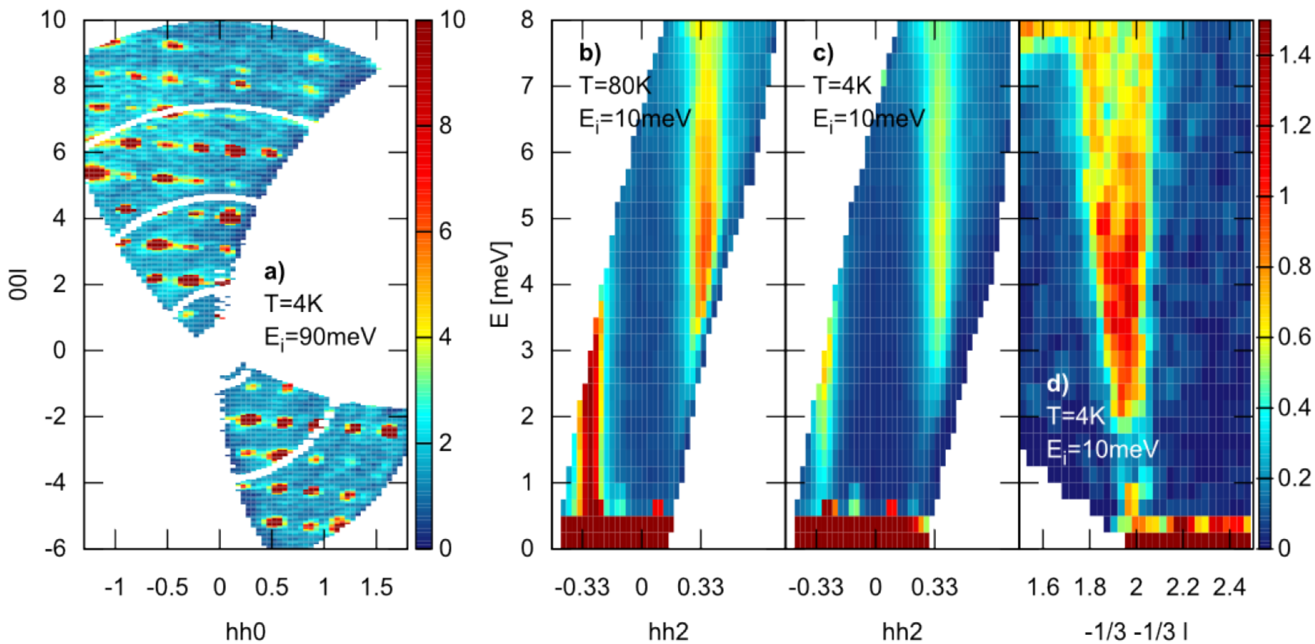

~ 10^5 n/s/cm^2 per "season"

$0.8\,\text{Å} < \lambda_i < 2.6\,\text{Å}$

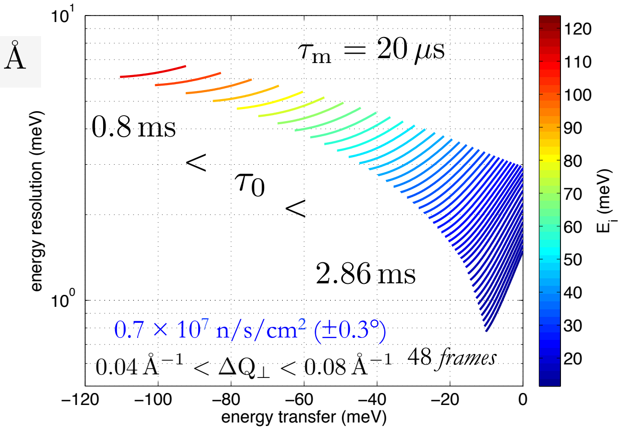

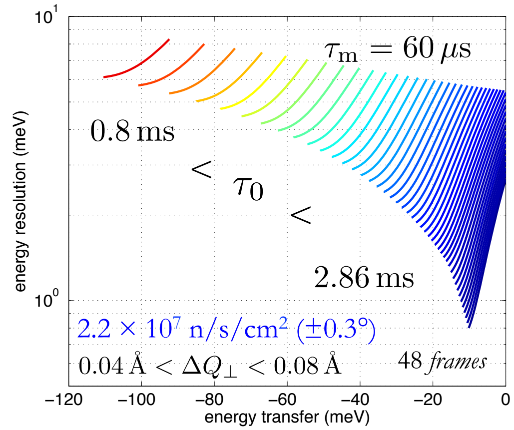

Resolution chopper

48x14Hz=672Hz

20µs

d=280µm

L=6.6mm

=>2.4°

Pulse selection

96,48,32,24

$2.0\,\text{Å} < \lambda_i < 3.8\,\text{Å}$

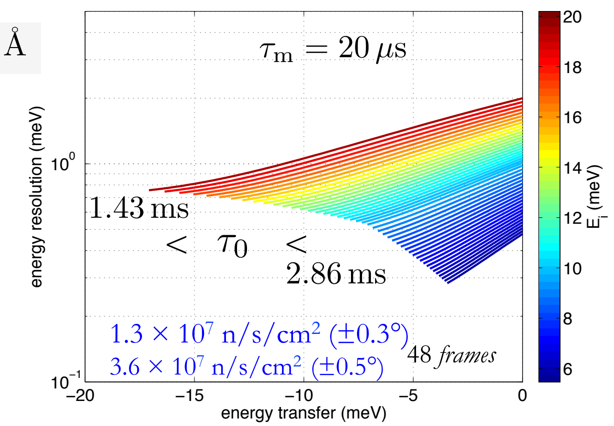

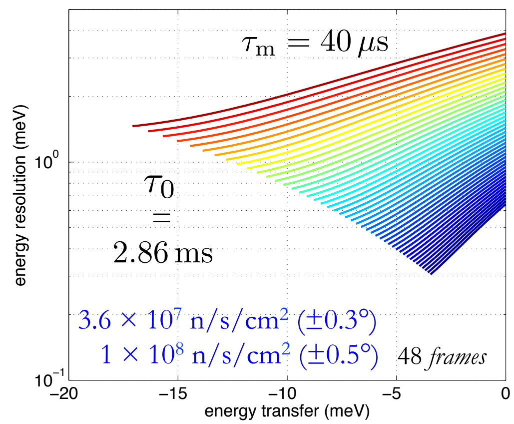

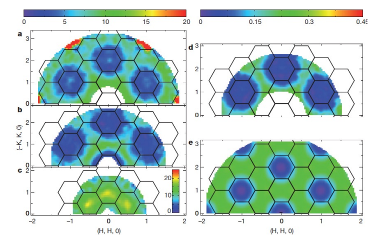

$4.0\,\text{Å} < \lambda_i < 5.8\,\text{Å}$

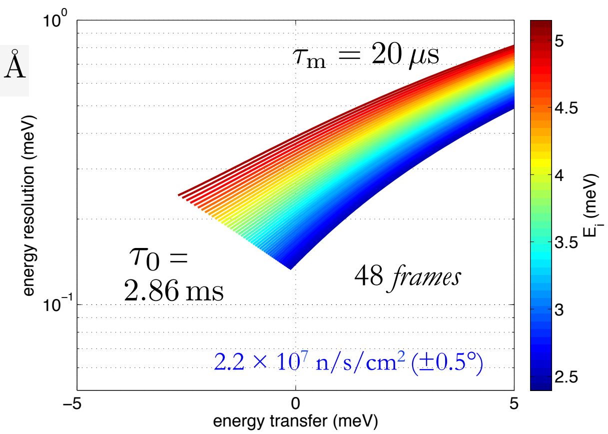

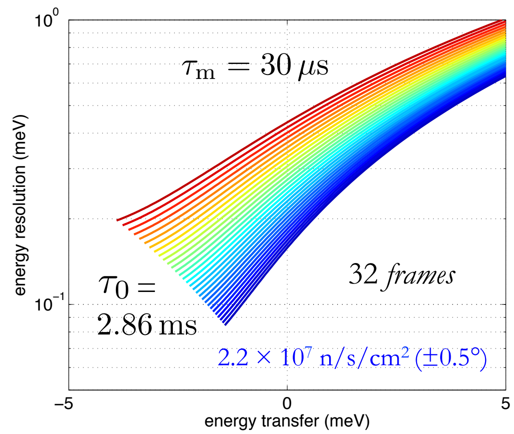

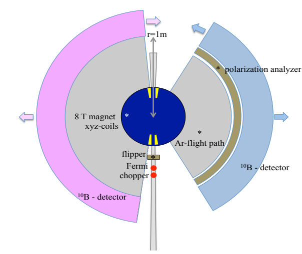

$0.8\text{Å} < \lambda < 2.65\text{Å}$ $\qquad$ $2.0\text{Å} < \lambda < 3.85\text{Å}$

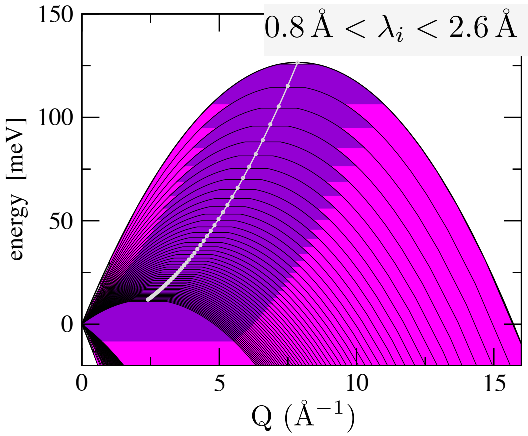

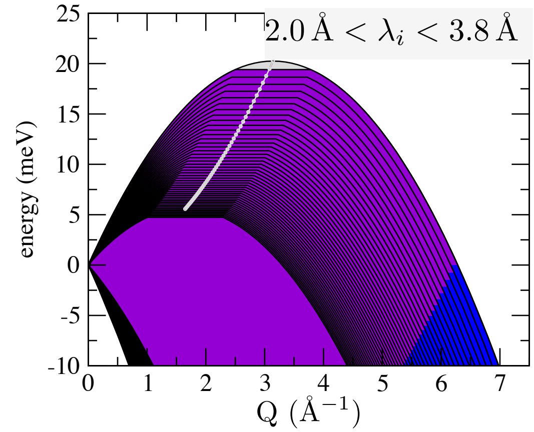

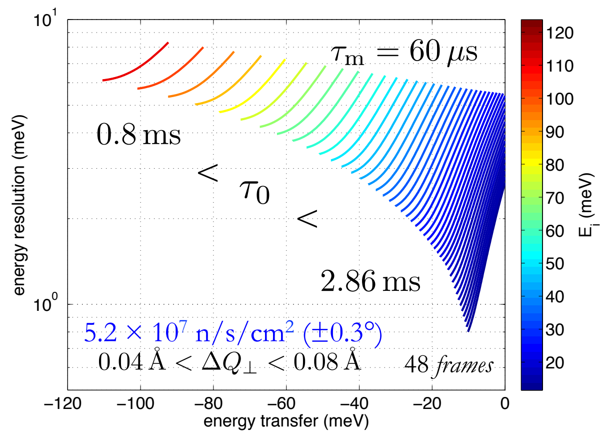

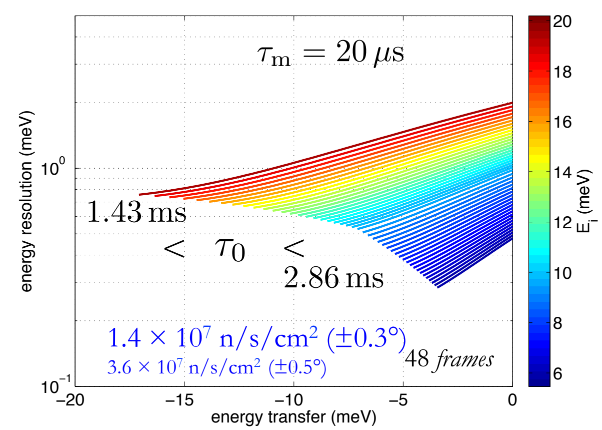

Gain: $\quad \tau_0 \, \tau_m \, 48 \;\; (\text{TOF} - \text{frames})$

Signal to background

Challenges to measure weak signals

epitaxial systems, weak moments, …

comparable or better than background of a (polarized) TAS instrument?

- Neutron guide curved+kinked, alternative Selene
- avoid material in primary beam
- Ar-flight paths
- Polarization analyzer
- minimize view detector view to sample
- pulsed time structure
- high polarization
- Volume detector – signal tracing to sample
- Global optimization MCNPX +McStass

Instrument performance and comparison

D3, D23, 6T2: We shall not make any comparisons in terms of gain factors to these single detector instruments. MAGiC will offer most of the experimental capabilities to serve the user communities of these instruments. Possible needs for higher than 8T vertical field will be covered by upgrades of instrument.

TAS/4C D10, IN12, … large gain compared to these single detectors, -> signal to background

DNS is an instrument for diffuse neutron scattering using a multi-detector and polarization analysis using cold monochromatic neutrons within 2.4Å<λ<6.2Å. The polarized flux is 10^7 n/s/cm^2. The incoming beam divergence at sample is 2°(horizontal) x 3°(vertical). The accepted divergence is 2°(horizontal) x 7°(vertical). The detector area is 0.1sr with PA, 3sr without PA. The flux gain is 280, better divergence gives a quality gain factor of ~10, solid angle coverage with PA yields a gain factor 2, resulting in a total gain factor larger than 3 orders of magnitude.

D7 is similar to DNS using cold monochromatic neutrons of λ=3.1Å, 4.8Å, or 5.7Å. The maximal polarized flux is 2x10^6 n/s/cm^2. The incoming beam divergence at sample is 2°(horizontal) x 3°(vertical). The accepted divergence is 2°(horizontal) x 7°(vertical). The detector area is 0.41sr with PA. The flux gain for MAGiC is larger than 1000, better divergence gives a quality gain factor of ~10, solid angle coverage with PA yields a loss factor of 0.7, resulting in a total gain factor larger than 3 orders of magnitude.
Both **DNS** and **D7** can operate in an inelastic mode as a DG-TOF spectrometer with polarization analysis. Comparing the performance for the inelastic case shows gain factors for MAGiC similar or higher to the diffraction case. One may add that particularly in view of the core science case of diffuse magnetic scattering with PA, the position sensitive detector of MAGiC will offer in addition valuable 3 dim Q-information and its detector-analyzer system will enable to measure Bragg- and diffuse intensities in Laue mode.

VIP: The monochromatic diffractometer VIP at LLB has a similar Heussler polarizer but it operates with a 2D position sensitive detector. It covers a Q-space 1.8 times smaller than MAGiC due to a smallest detector and higher wavelength. The raw flux at λ=1.2 Å of VIP at sample position is of 10^7 n/s/cm^2. Comparing to the thermal MAGiC flux, the gain is about 100 and we estimate a total gain of 200.

DREAM: optimized for powder diffraction, for unpolarized single crystal diffraction actually better performing than MAGIC because of a larger detector

NMX: optimized only for structure determination of large unit cellls. Anisotropic resolution ellipsoid: $Q_{||}$ poor and Q_{perp} brilliant. Lack of thermal neutrons.

HYSPEC is a similar to DNS and D7 a multi-detector instrument with polarization analysis, however, it is a dedicated crystal-TOF for inelastic studies. It uses a Heussler monochromator yielding a pulsed monochromatic flux of 7×10^4 n/s/cm^2 with $\Delta E_i/E_i$=0.06 at E_i=15 meV. The detector coverage with PA is ~0.4sr. The incoming beam divergence at sample is 0.8°(horizontal) x 2.4°(vertical). The accepted divergence is 2°(horizontal) x ~5°(vertical). At this energy resolution and energy range the instrument MAGiC will have a flux of 2.8×10^7 n/s/cm^2 (gain 400), however, with better divergence definition of 1.0°x1.0° and Q-resolution, yielding a further quality gain factor of (~10), resulting in a total gain factor larger than 3 orders of magnitude.

4SEASONS is a new high-performing DG-TOF instrument at JPARC using simultaneously 4 incident wavelengths. 4SEASONS is an unpolarized instrument with a flux of 1×10^5 n/s/cm^2 with $\Delta E_i/E_i$=0.05 at E_i=50meV. A comparison to the inelastic option of MAGiC, which uses 48 λ_i's of the polarized thermal spectrum, yields 2.2×10^7 n/s/cm^2 with $\Delta E_i/E_i$=0.07, and we compare for similar solid angle of detection using the large detector without PA. The total gain is larger than 2 orders of magnitude (without taking the advantage of polarization at MAGiC into account).

ESS: VOR (wide band width ~10 frames) and TREX (narrow bandwidth ~<20 frames) have roughly similar performance to 4SEASONS for each monochromatic pulse with better resolution possible.

Neutron TOF Laue using the proposed powder diffractometer DREAM

unpolarized   0.6Å < λ < 10Å
large solid angle

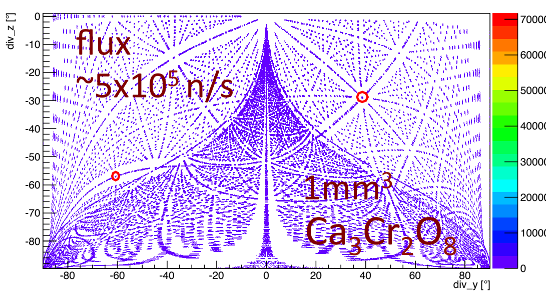

tuneable resolution element
flexible high time resolution

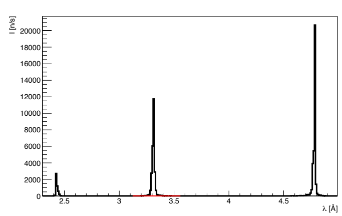

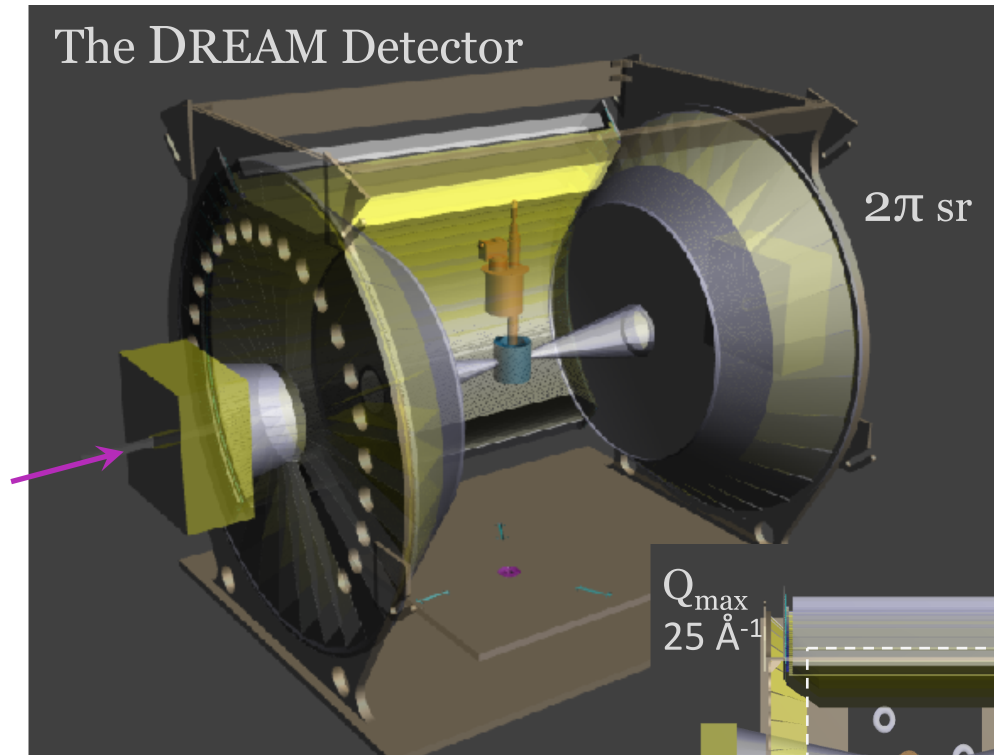

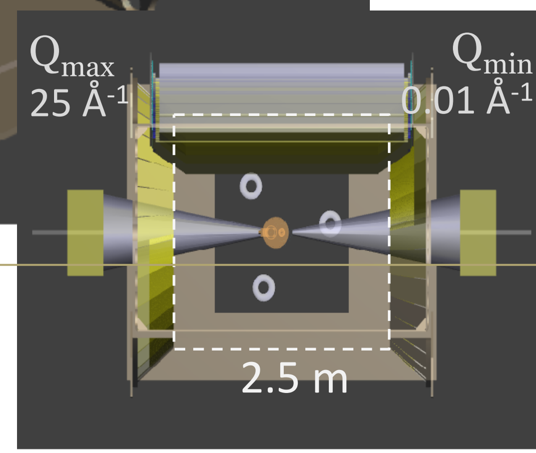

- little blind sections
- top *and side* access
- new B-10 detector is a 1 bar volume multi-wire chamber
  CDT-PowTex-prototype tested, 55% efficiency at 1 Å
  3 to 4 mm resolution, very high count rate capability
  new opportunities to improve signal to background

Simulation of the
NMX instrument at ESS

Neutron TOF Laue
for macromolecular crystallography
(Esko Oksanen)

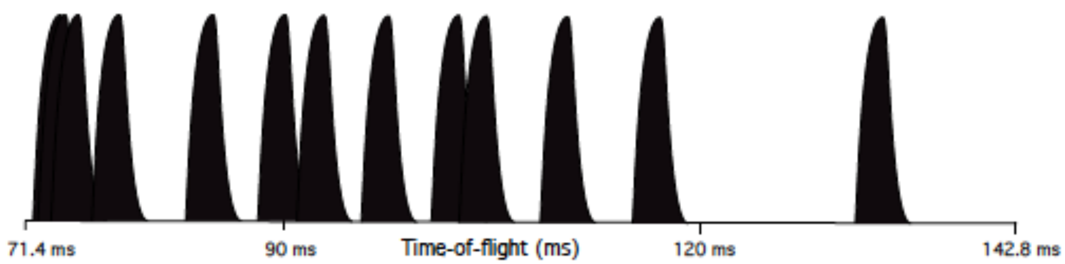

separation of peaks in time
using full pulse width gain ~ 10^2

anisotropic resolution element
time resolution given by ESS pulse
separates sufficiently higher order Bragg peaks